

Supporting Information

Polytype selection in the antisolvent-free crystallization of formamidinium lead iodide using alkylammonium chlorides

*Paulo E. Marchezi^{1,‡}, Jack R. Palmer^{2,‡}, Maimur Hossain¹, Tim Kodalle^{3,4}, Raphael F. Moral^{3,5},
Carolyn M. Sutter-Fella³, David P. Fenning^{1,2*}*

¹Aiiso Yufeng Li Family Department of Chemical and Nano Engineering, University of California San Diego, 9500 Gilman Drive, La Jolla, California 92093, United States.

²Materials Science & Engineering Program, University of California San Diego, 9500 Gilman Drive, La Jolla, California 92093, United States

³Molecular Foundry Division, Lawrence Berkeley National Laboratory, 1 Cyclotron Road, Berkeley, California 94710, United States.

⁴Advanced Light Source, Lawrence Berkeley National Laboratory, 1 Cyclotron Road, Berkeley, California 94710, United States.

⁵Nevada Extreme Conditions Laboratory, University of Nevada, Las Vegas, Las Vegas, Nevada 89154, United States

*Correspondence to: dfenning@ucsd.edu

Supplementary Note 1

The use of NH_4Cl as an additive illustrates the significant impact of additive volatility and ionic radius on the crystallization process. NH_4Cl , with its high volatile conjugated base and small ionic radius, leads to the early formation of the 3C perovskite structure around 72°C , as shown in supplementary data (Figure S2). This is consistent with literature reports indicating that volatile additives can promote rapid crystallization at lower temperatures.¹ However, the premature evaporation of NH_4Cl hinders the stabilization of the 3C phase, eventually leading to the formation of PbI_2 at higher temperatures (138°C). Such findings align with studies highlighting the challenge of maintaining phase stability when using highly volatile additives.¹

The behavior of NH_4Cl additive presents a distinct contrast in their influence on perovskite phase stability and degradation. In samples treated with NH_4Cl , the GIWAXS data (Figure S2) shows an initial increase in the PbI_2 peak intensity at the onset of annealing, coupled with a slight decrease in the 3C phase peak. This pattern suggests that the 3C FAPbI_3 phase undergoes degradation, likely due to the expulsion of NH_4Cl during the spin-coating process, which leaves the cubic phase without effective stabilization. The early appearance of PbI_2 and the reduction in the 3C phase indicate that NH_4Cl is not effective in maintaining phase stability under thermal stress.

Figure S1. GIWAXS of control films. Heat map of azimuthally integrated in situ GIWAXS over the FAPbI₃ film deposition process. (a) 0.0% NMP and no MACl. (b) 0.0% NMP and 15.0 mol% MACl. (c) 7.5% NMP and no MACl. All gray-dashed lines are heating curves.

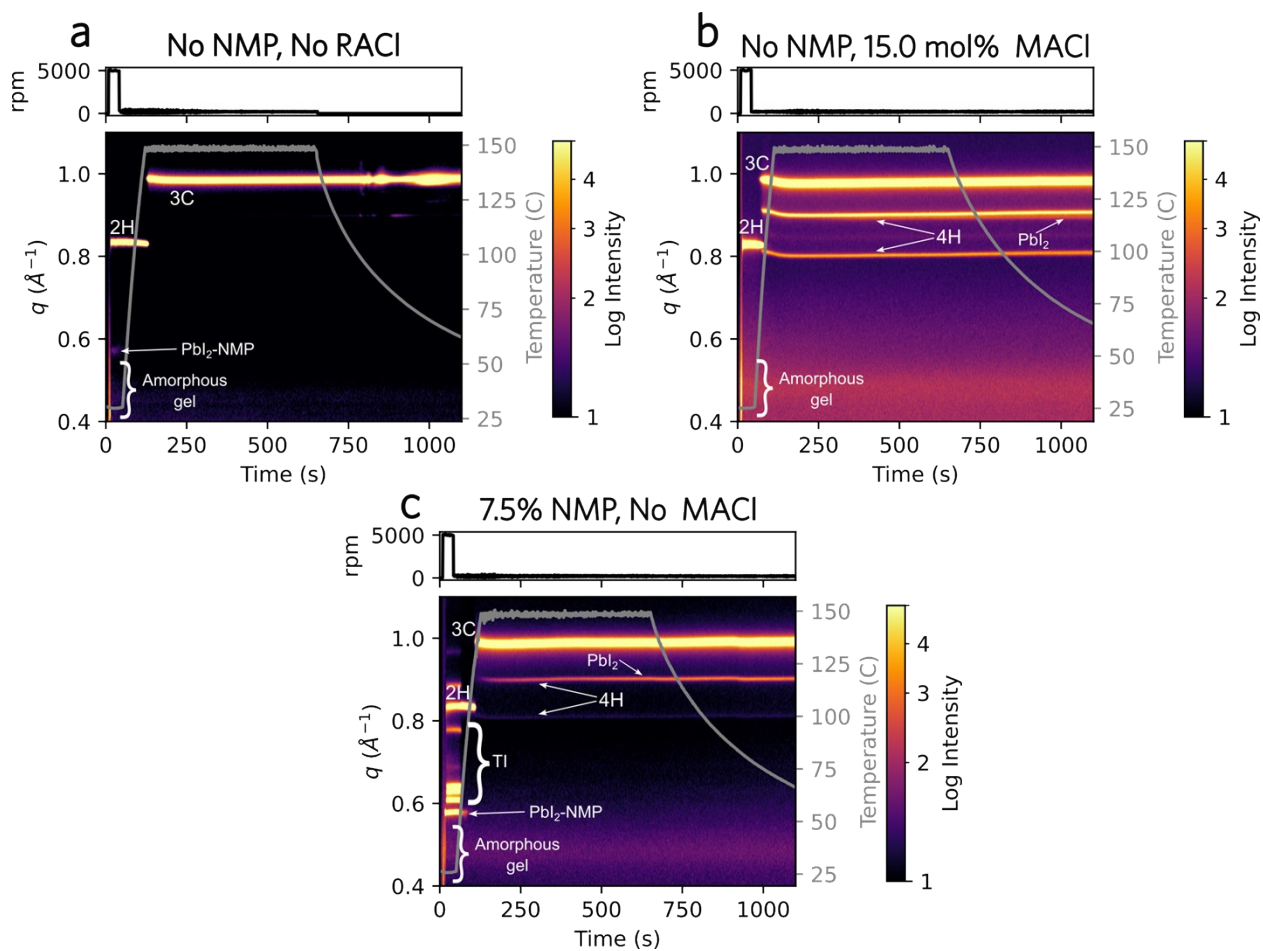


Figure S2. Heat map of azimuthally integrated in situ GIWAXS over the film deposition process. (a) 7.5 mol% NH_4Cl . (b) 15.0 mol% NH_4Cl . (c) 22.5 mol% NH_4Cl . All gray-dashed lines are heating curves.

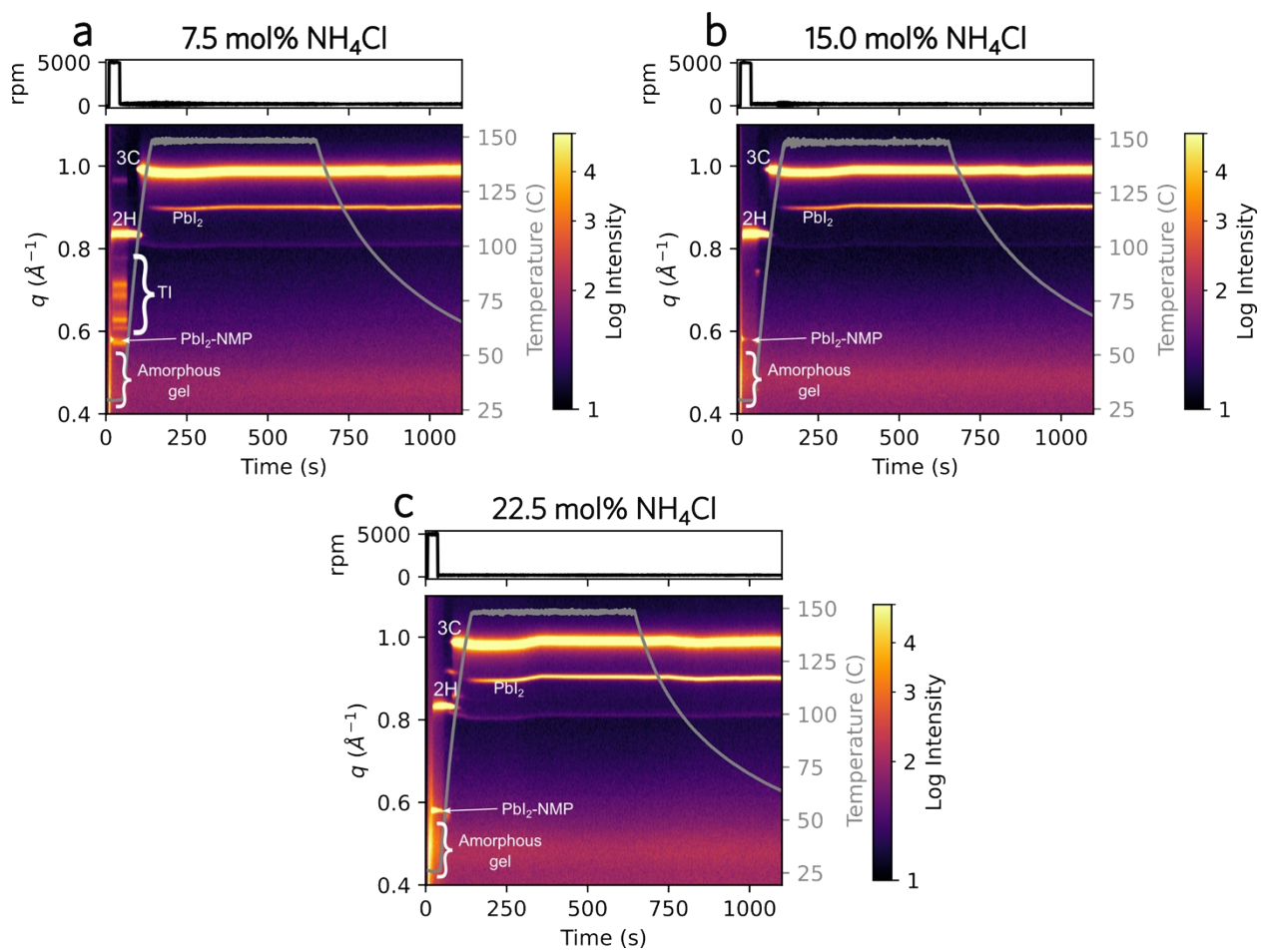


Figure S3. Heat map of azimuthally integrated in situ GIWAXS over the film deposition process. (a) 7.5 mol% MACl. (b) 15.0 mol% MACl. All gray-dashed lines are heating curves.

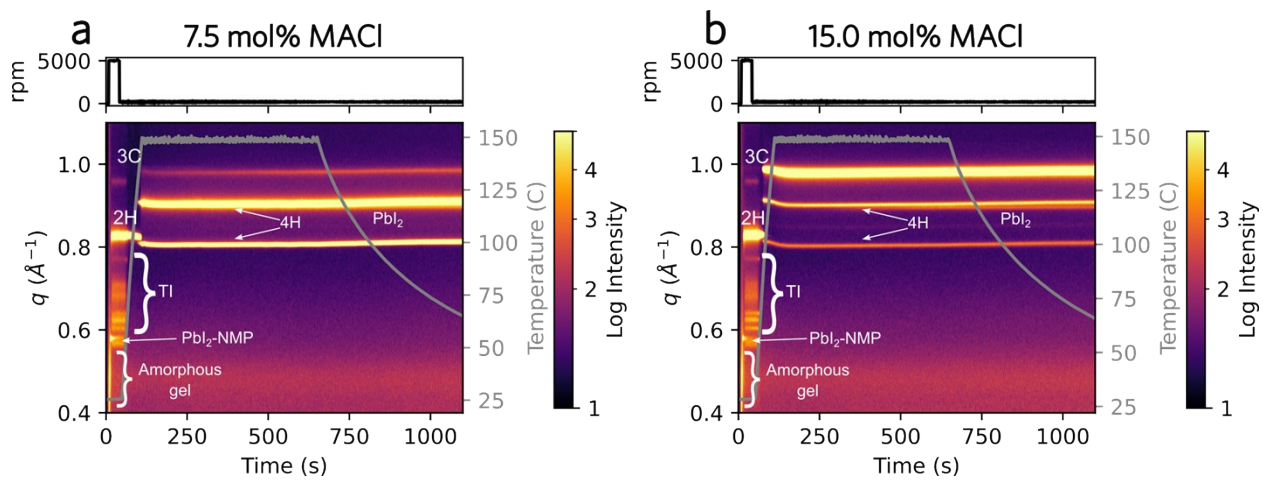


Figure S4. Heat map of azimuthally integrated in situ GIWAXS over the film deposition process. (a) 7.5 mol% EACI. (b) 15.0 mol% EACI. (c) 22.5 mol% EACI. All gray-dashed lines are heating curves.

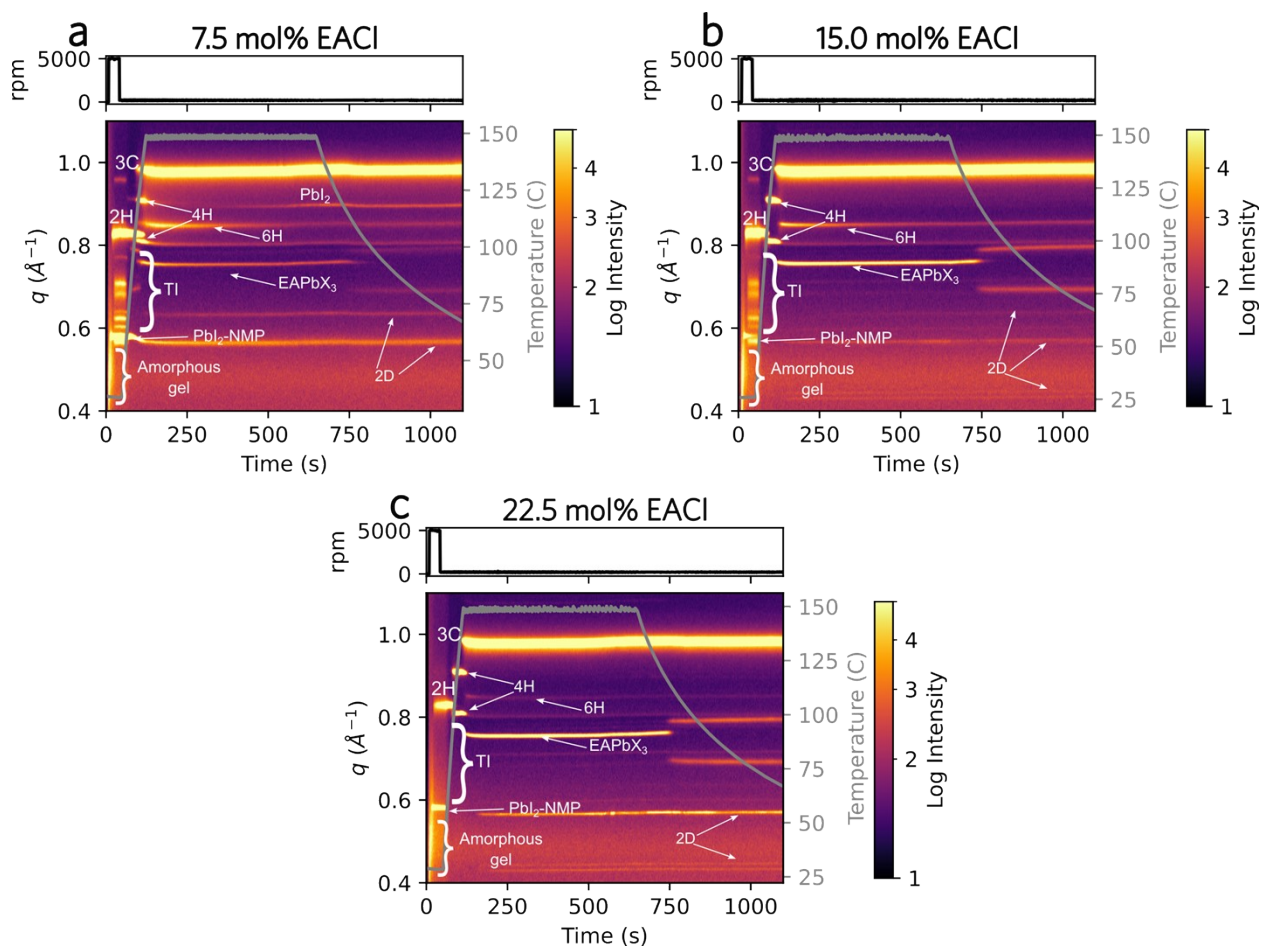


Figure S5. Heat map of azimuthally integrated in situ GIWAXS over the film deposition process. (a) 7.5 mol% iPACl. (b) 15.0 mol% iPACl. (c) 22.5 mol% iPACl. All gray-dashed lines are heating curves.

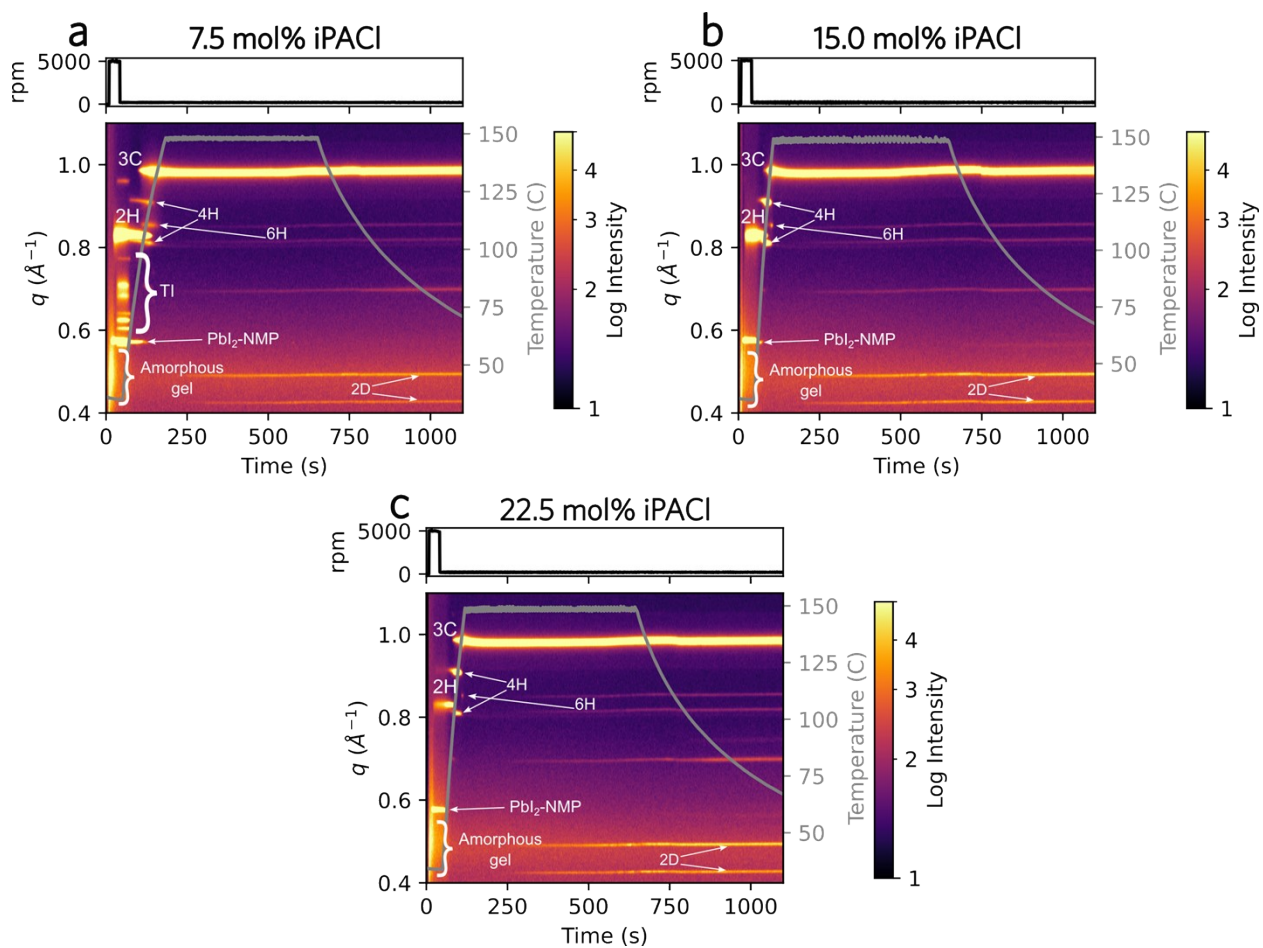


Figure S6. Heat map of azimuthally integrated in situ GIWAXS over the film deposition process. (a) 7.5 mol% nPACl. (b) 15.0 mol% nPACl. (c) 22.5 mol% nPACl. All gray-dashed lines are heating curves.

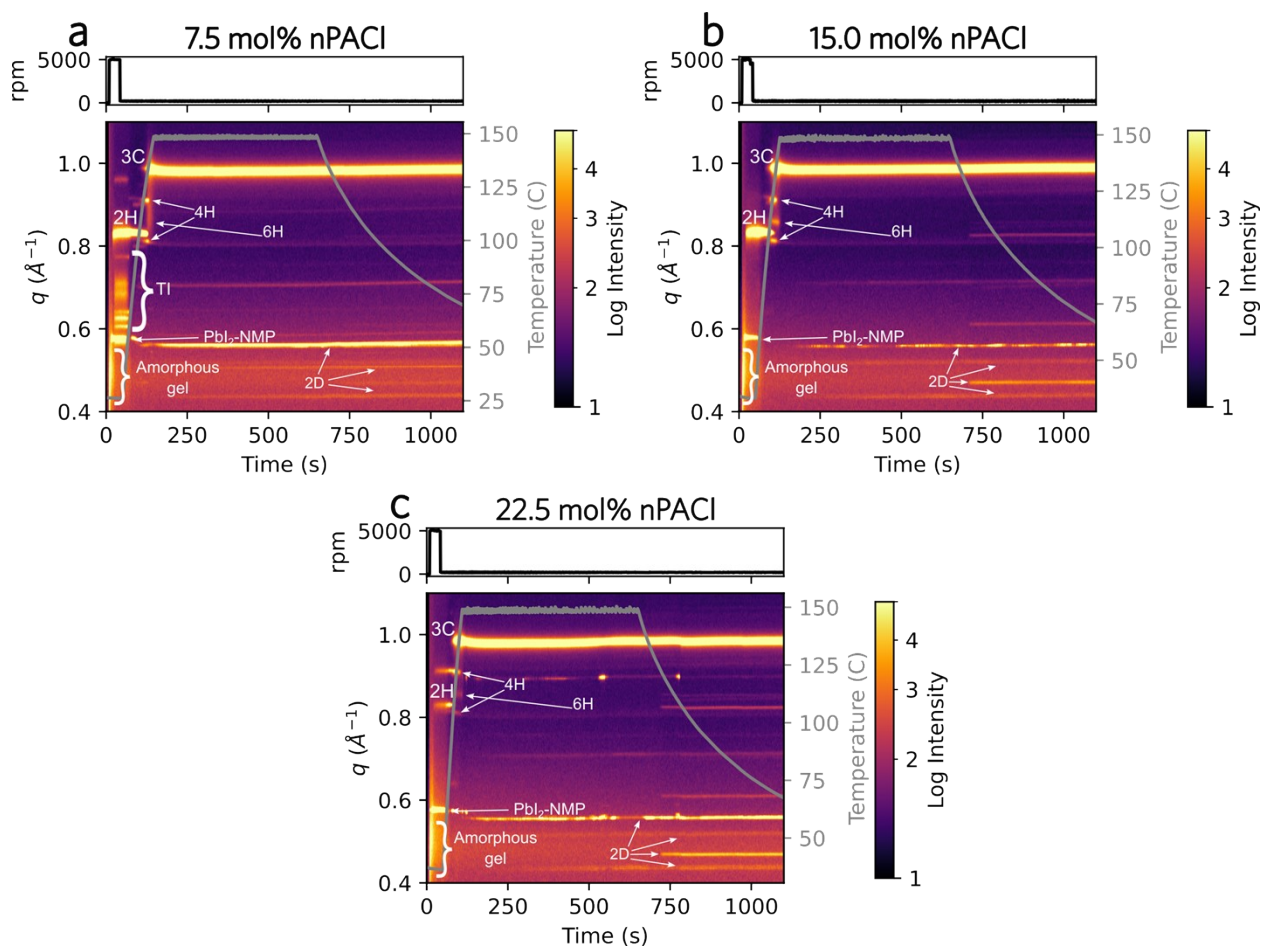


Figure S7. Heat map of azimuthally integrated in situ GIWAXS over the film deposition process. (a) 7.5 mol% nBACl. (b) 15.0 mol% nBACl. (c) 22.5 mol% nBACl. All gray-dashed lines are heating curves.

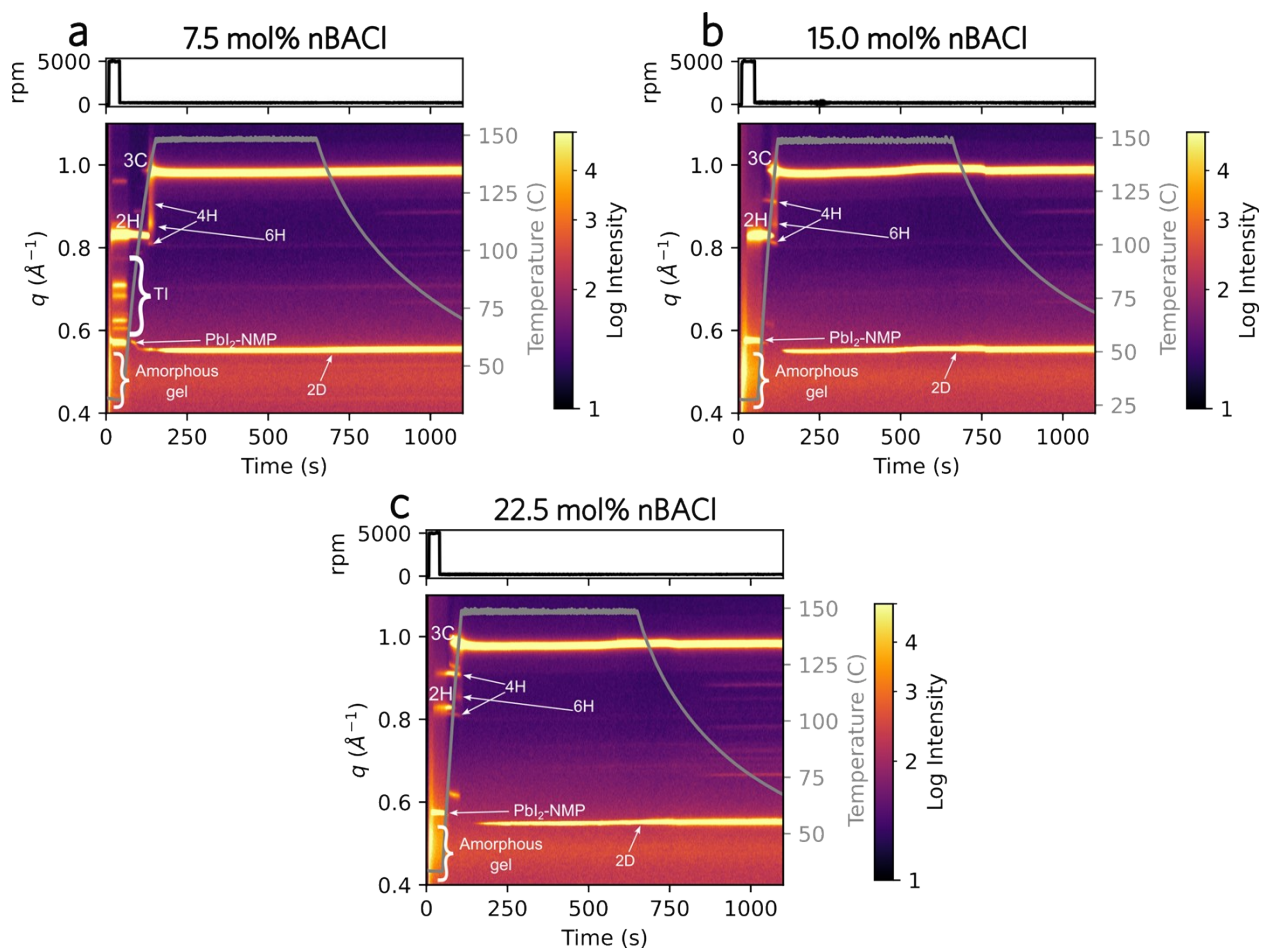


Figure S8. 2D GIWAXS data acquired for Control sample with no additive (a), with 15.0 mol% of NH_4Cl (b), MACl (c), EACl (d), iPACl (e), nPACl (f), and nBACl (g)

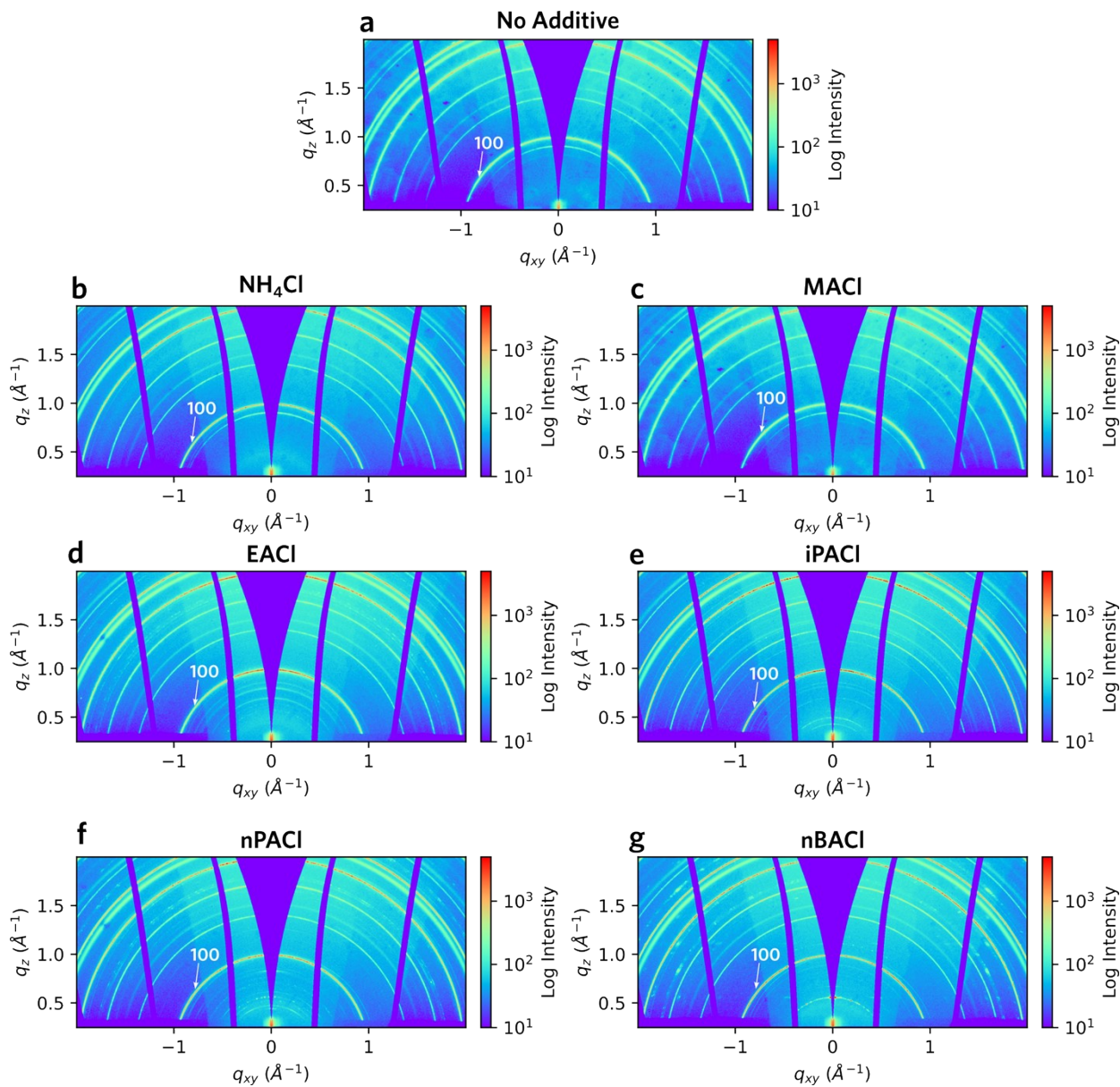


Figure S9. Azimuthal intensity profiles of the (001) perovskite reflection for samples prepared with 15% mol. (a) NH_4Cl , (b) MACl , (c) EACl , (d) iPACl , (e) nPACl , and (f) nBACl . 300 diffraction images were averaged to improve signal-to-noise.

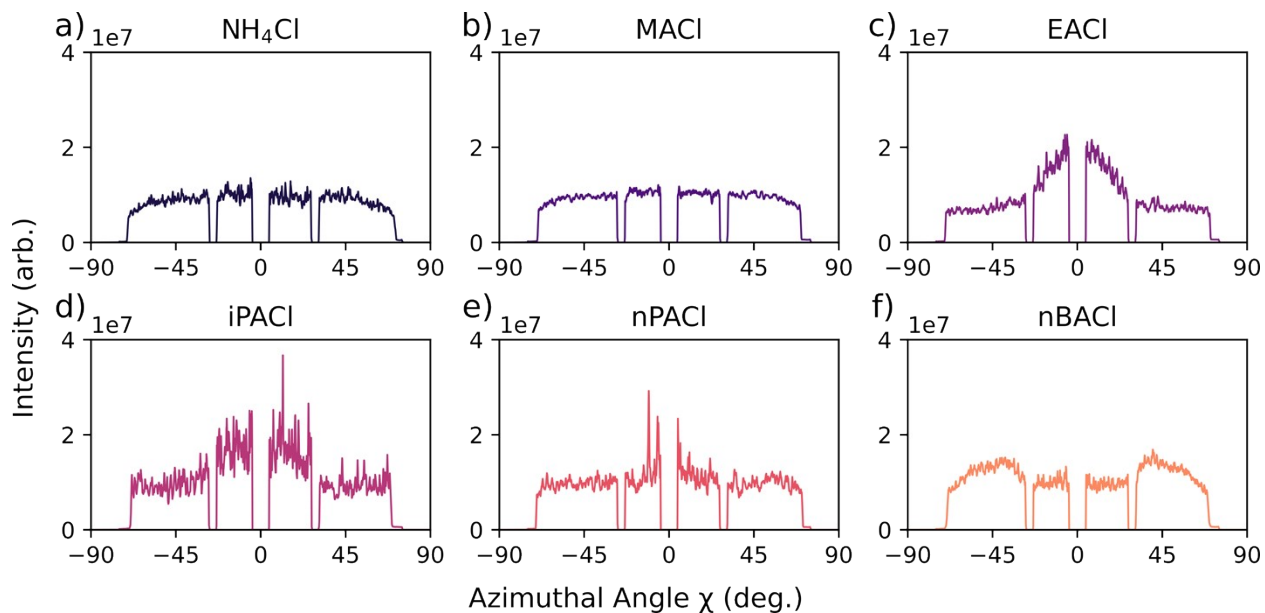


Figure S10. Representative PL spectra of perovskite films modified with 15.0 mol% of a) NH_4Cl , b) MACl , c) EACl , d) iPACl , e) nPACl , and f) nBACl .

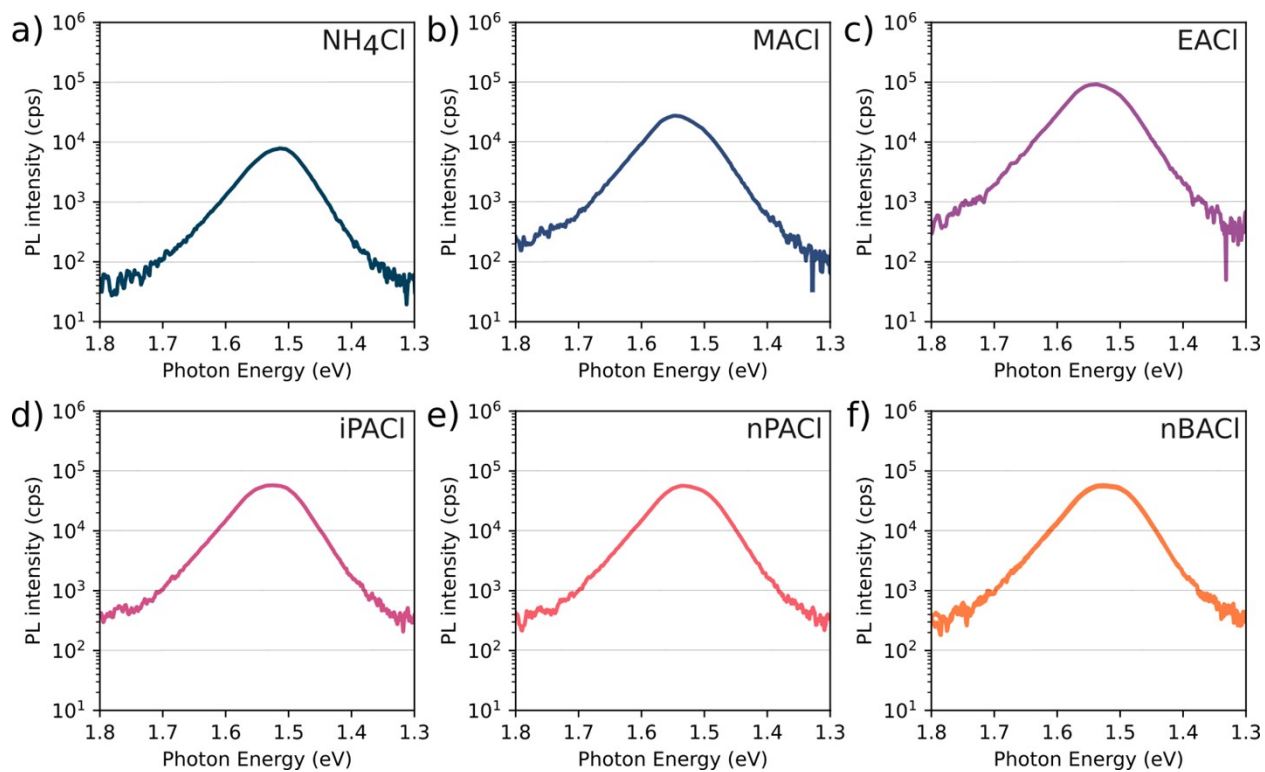
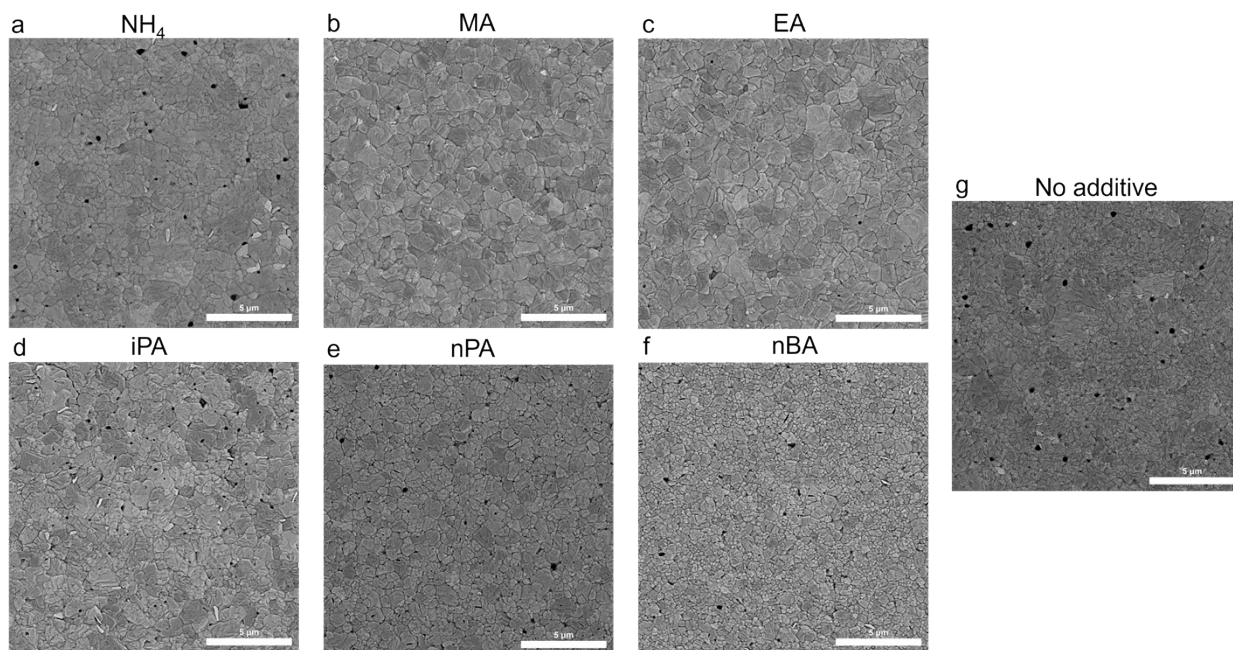


Figure S11. SEM images spectra of perovskite films modified with (a) 15.0 mol% of NH_4Cl , (b) MACl , (c) EACl , (d) iPACl , (e) nPACl , (f) nBACl , and (g) No additive. Scale bar, 5 μm .



Supporting References

- (1) Bi, L.; Fu, Q.; Zeng, Z.; Wang, Y.; Lin, F. R.; Cheng, Y.; Yip, H.-L.; Tsang, S. W.; Jen, A. K.-Y. Deciphering the Roles of MA-Based Volatile Additives for α -FAPbI₃ to Enable Efficient Inverted Perovskite Solar Cells. *J. Am. Chem. Soc.* **2023**, *145* (10), 5920–5929. <https://doi.org/10.1021/jacs.2c13566>.